Multiple-electron removal and molecular fragmentation of CO by fast F^{4+} impact

I. Ben-Itzhak, S. G. Ginther, and K. D. Carnes
James R. Macdonald Laboratory, Department of Physics, Kansas State University, Manhattan, Kansas 66506
(Received 21 May 1992)

Multiple-electron removal from and molecular fragmentation of carbon monoxide molecules caused by collisions with 1-MeV/amu F^{4+} ions were studied using the coincidence time-of-flight technique. In these collisions, multiple-electron removal of the target molecule is a dominant process. Cross sections for the different levels of ionization of the CO molecule during the collision were determined. The relative cross sections of ionization decrease with increasing number of electrons removed in a similar way as seen in atomic targets. This behavior is in agreement with a two-step mechanism, where first the molecule is ionized by a Franck-Condon ionization and then the molecular ion dissociates. Most of the highly charged intermediate states of the molecule dissociate rapidly. Only CO^+ and CO^{2+} molecular ions have been seen to survive long enough to be detected as molecular ions. The relative cross sections for the different breakup channels were evaluated for collisions in which the molecule broke into two charged fragments as well as for collisions where only a single charged molecular ion or fragment were produced. The average charge state of each fragment resulting from $CO^{Q+} \rightarrow C^{i+} + O^{j+}$ breakup increases with the number of electrons removed from the molecule approximately following the relationship $\bar{i} = \bar{j} = Q/2$ as long as K-shell electrons are not removed. This does not mean that the charge-state distribution is exactly symmetric, as, in general, removing electrons from the carbon fragment is slightly more likely than removing electrons from the oxygen due to the difference in binding energy. The cross sections for molecular breakup into a charged fragment and a neutral fragment drop rapidly with an increasing number of electrons removed.

PACS number(s): 34.50.−s, 35.80.+s, 34.90.+q

I. INTRODUCTION

The fragmentation process of molecular ions has been investigated mostly for photoionization and electron-impact processes. In these processes one electron of the target molecule is ionized, resulting in some dissociating states. A small fraction of the molecules will be doubly ionized, and this process has been studied using coincidence between the two fragments to distinguish this small breakup channel from the main single-ionization channel. Electron-impact ionization studies have been performed since the pioneering work of McCulloh and Rosenstock [1]. Brehm and Frenes performed extensive studies of ion-pair formation in electron impact processes on diatomic molecules [2] in which they determined the threshold energy for ion-pair formation, the kinetic energy of the fragments, and their intensity relative to the total ion count. Since the development of high intensity light sources, such as synchrotron radiation sources, molecular fragmentation induced by photoionization has been of increasing interest. For example, the dissociation of carbon monoxide, which is the molecule of interest in this work, has been studied by Lablanquie *et al.* [3,4] over the photon energy range of 35–150 eV. In this energy range fragments originating from CO^{2+} and CO^{3+} have been seen. The dominant breakup path of the triply ionized molecule is the formation of the $C^{2+}+O^+$ ion pair while the doubly ionized molecule breaks mainly into $C^+ + O^+$. These studies were extended by Hitchcock *et al.* [5] to K-shell photoionization by using higher energy photons, which create an inner-shell vacancy on either the carbon or the oxygen. A rapid Auger process follows in which one or a few electrons are ionized leading to highly charged molecular ions.

The fragmentation of diatomic molecules caused by light ion impact, namely, H^+ and He^{2+} ions, has been studied by Edwards and Wood [6]. Recently, the fragmentation of carbon monoxide caused by light ion impact was studied by Shah and Gilbody [7]. In these collisions the target electrons can be removed by either ionization or capture. The number of electrons removed from the target molecule decreases rapidly for all the processes described above such that only the breakup of low-charge states of CO can be studied.

It is well established that fast highly charged ion impact is a very efficient method for creating highly charged target atoms. (See, for example, Cocke [8].) This is also the case for molecular targets. (See, for example, Tawara's observations of N^{6+} fragments resulting from N_2 dissociation [9].) Direct evidence of multiple ionization of O_2 in collisions with 1-MeV/amu Ar^{13+} ions was reported by Sampoll *et al.* [10]. Recently, Sampoll *et al.* [11] reported on the dissociation of multicharged carbon monoxide ions produced by 2.425-MeV/amu Ar [14] impact. The kinetic-energy distribution of the outgoing ion pairs has been evaluated from the coincidence time-of-flight (TOF) spectra.

In this paper we report the studies of carbon monoxide fragmentation caused by 1-MeV/amu F^{4+} impact. The coincidence time-of-flight technique and the experimental apparatus used for these studies have been described in detail elsewhere [12]. The experimental method is dis-

cussed briefly in Sec. II. Our work has focused on the determination of the relative importance of the different breakup channels and on the electron-removal cross sections. The evaluation of these relative abundances and cross sections is presented in Sec. III, with details of the calculations given in the Appendix. The fragmentation process has been found to peak approximately at $\bar{j}=Q/2$. Electron-removal cross sections decrease rapidly with increasing number of electrons removed approximately at the same rate for both CO and Ne targets as discussed in Sec. IV.

II. EXPERIMENTAL METHOD

The experimental setup used in our molecular fragmentation studies, shown in Fig. 1, was described in detail in a previous publication [12]. Briefly, a bunched beam of F^{4+} ions was accelerated in the J. R. Macdonald Tandem Van de Graaff accelerator to an energy of 19 MeV. The collimated beam was then directed into a target cell containing the target gas through a 1.5-mm-diameter collimator which guided the beam through the target center. After passing the collision region the beam was collected in a Faraday cup down stream for normalization. The bunched beam technique for time-of-flight studies was chosen over the projectile-recoil coincidence technique as it allows the measurement of processes having smaller cross sections by about three orders of magnitude. A manually controlled leak valve was used to maintain constant pressure in the gas cell. This pressure was monitored by a capacitive manometer and was kept below 0.1 mTorr to insure single-collision conditions.

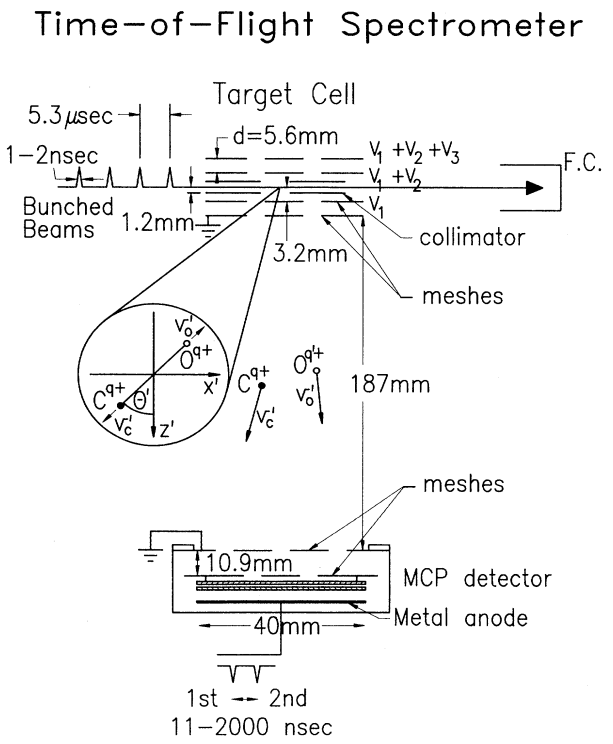

FIG. 1. Experimental setup used for coincidence time-of-flight spectroscopy. FC denotes a Faraday cup and MCP a microchannel-plate detector.

Ions produced in the collision region were extracted by a strong uniform electric field $\mathcal{E}_2$ between the center meshes. The ions passed through a second uniform electric field $\mathcal{E}_1$ which accelerated them into a field free region, where they drifted into a large chevron microchannel-plate detector. The ratio $k=V_1/V_2$ between the time-of-flight spectrometer voltages was set to give the best space focusing (i.e., the same times of flight for ions produced at rest anywhere within the collision region), following the Wiley and McLaren [13] condition. The minimum time resolution $\Delta t/t$ for Ne^+ ions, which typically have thermal energies (~ 0.04 eV) in these collisions [14], was found to be 2.5×10^{-3} independent of V_2 as expected. A large square (6×6 mm^2) aperture in a thin (0.0254-mm) metal foil, which was held at the proper voltage using a resistor chain between the center meshes, served as the exit collimator for the recoils. This collimator defines a collision region from which ions can be extracted. This effective target length $l_T=6$ mm is independent of the beam trajectory through the target cell. The collimator was placed as close as possible to the beam trajectory ($d_c\sim1.2$ mm) in order to maximize the efficiency for ion-pair extraction. Special care was taken to insure the uniformity of the electric fields. A large detector (40-mm diameter) was needed to insure that for the strong extraction field used all the ions extracted through the collimator would hit the detector, thus minimizing angular discrimination effects. These angular discrimination effects must be considered especially carefully for molecular fragmentation caused by multiple ionization, since the kinetic energy released in such fragmentation is large. Kinetic energies of above 100 eV were measured for multiply ionized CO in comparison to about 10 eV typically measured in the dissociation of doubly charged CO.

The times of flight of all ions hitting the detector were recorded by a time-to-digital converter (LeCroy model 4208) in multiple hit mode. A fast timing signal synchronized with the beam bunch was used as a common start while the signals created by the recoil ions were used as the stops. The time difference between each recoil and the common signal was recorded event by event so as to maintain the correlation between all times of flight associated with the same beam bunch. The discriminator level of the constant-fraction-discriminator, which produced the recoils signal, was set low enough to insure that the singly charged ions, which have a relatively small signal, were not lost. (This was verified by measuring the relative yields for multiple ionization of neon atoms by highly charged fluorine ions and comparing to previous measurements by Gray, Cocke, and Justiniano [15].)

III. DATA ANALYSIS

Fragmentation of CO caused by collisions with F^{4+} ions at 1 MeV/amu was studied. Multiple ionization is expected to be important in these collisions [8–12], creating highly charged intermediate states of the molecule.

These unstable states dissociate rapidly into two charged fragments (ion-pair channels) or a single charged fragment and a neutral fragment (single-ion channels). The kinetic energy carried by these fragments increases with their charge states and is relatively high in comparison with energies associated with the breakup of singly and doubly charged CO. Our goal is to determine the relative abundances of all breakup channels and their cross sections.

The spectrum of events in which only a single recoil ion was detected are presented in Fig. 2. It can be seen that the molecular-ion peaks, i.e., CO^+, CO^{2+}, and H_2O^+ are much narrower than the peaks of the fragments. The time broadening of the fragment peaks is due mainly to the kinetic energy released in the breakup process. On the other hand the time broadening of the molecular ions is due mainly to thermal motion. The differences in width indicate that the breakup kinetic energies are much larger than the ~0.04-eV energy of the thermal motion. Both these contributions to the time broadening are significantly larger than the beam bunch width (<1.5 nsec) or the broadening due to the electronic system which was about 1.1 nsec. The high charge states detected as single fragments are believed to be due to events where two charged fragments were formed in the collision but only one of them was detected due to the fact that the recoil detection efficiency is less than one. For example, a CO^{7+} which breaks into a C^{4+} and O^{3+} will be detected as a coincidence event with a certain detection efficiency. The same event might contribute to the yield of C^{4+} or O^{3+} single ions if the other fragment was not detected. These contributions have to be subtracted from the single-fragment spectrum in order to evaluate the cross sections of all the channels where only one charged fragment was formed.

The different breakup channels of CO into two charged fragments can be identified in the coincidence spectrum shown in Fig. 3 as a three-dimensional (3D) plot of intensity versus t_1 and t_2, where t_1 and t_2 are the times of flight of the first and second fragment, respectively. A few breakup channels measured in coincidence are identified on the figure by their times of flight t_1 and t_2. In addition to the lost fragments corrections necessary for the single channels the coincidence channels also require corrections for random coincidences. Both singles and coincidence data must be corrected for contaminants in the target gas. All of these corrections to the single-fragment and ion-pair rates are coupled to one another. Details of the coupling and the corrections themselves can be found in the Appendix.

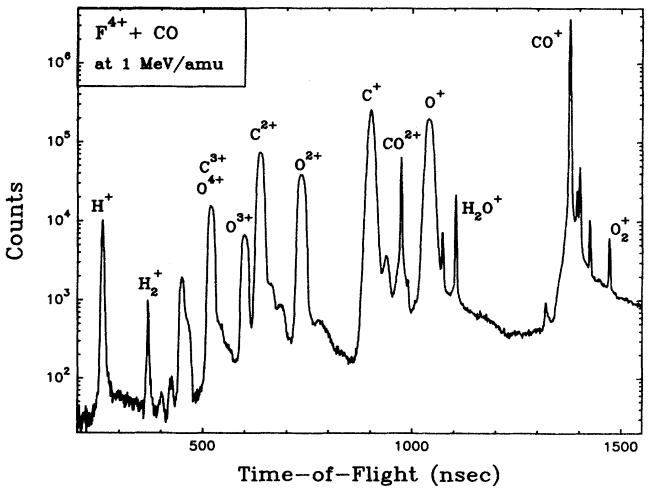

FIG. 2. TOF single-fragment spectrum of CO fragmentation, produced by F^{4+} impact at 1 MeV/amu, measured with a strong extraction field of 1250 V/cm.

Once corrections are made for the true number of single-fragment and ion-pair events, the relative abundances and cross sections of the different channels can be evaluated as described below. Refer to the Appendix for a complete definition of symbols. The abundances of all single channels relative to the singly charged molecular ion CO^+, given for example for $C^{i+}+O$ breakup by

$$\sigma_{\rm rel}(C^{i+})=\frac{\sigma(C^{i+})}{\sigma(CO^+)}=\frac{S(C^{i+})}{S(CO^+)}=\frac{S_e(C^{i+})}{S_e(CO^+)}\ , \quad (1)$$

are tabulated in Table I. S refers to the number of true single ions produced, and $S_e=\epsilon_r S$, where ϵ_r is the detection efficiency of a recoil ion. The abundances of all ion-pair breakup channels relative to the largest ion-pair breakup channel C^++O^+ given by

$$\sigma'_{\rm rel}(C^{i+},O^{j+})=\frac{\sigma(C^{i+},O^{j+})}{\sigma(C^+,O^+)}=\frac{C(C^{i+},O^{j+})}{C(C^+,O^+)}=\frac{C_e(C^{i+},O^{j+})}{C_e(C^+,O^+)}\ , \quad (2)$$

are tabulated in Table II. C refers to the number of true ion pairs produced, and $C_e=\epsilon_r^2 C$.

In order to compare the single-fragment channels to the ion-pair channels it is necessary to define all these abundances relative to the same quantity. The natural choice is the CO^+ molecular ion which is the main final product. These abundances relative to CO^+, given by

$$\sigma_{\rm rel}(C^{i+},O^{j+})=\frac{\sigma(C^{i+},O^{j+})}{\sigma(CO^+)}=\frac{C(C^{i+},O^{j+})}{S(CO^+)}=\frac{C_e(C^{i+},O^{j+})}{\epsilon_r S_e(CO^+)}\ , \quad (3)$$

are tabulated in Table III along with the single relative abundances. The ion-pair cross sections relative to CO^+ have a larger error due to the additional ϵ_r in Eq. (3). Thus, whenever comparing ion-pair channels to each other it is more accurate to use the values in Table II. On the other hand, the less accurate values given in Table III have to be used when single-fragment channels and ion-pair channels are used together, for example when evaluating the cross sections for removing a certain number of target electrons.

The total cross section for CO^+ production by 1-MeV/amu F^{4+} impact was evaluated by measuring the yield of CO^+ relative to the yield of Ne^+ produced by the same projectiles under the same conditions, i.e., the

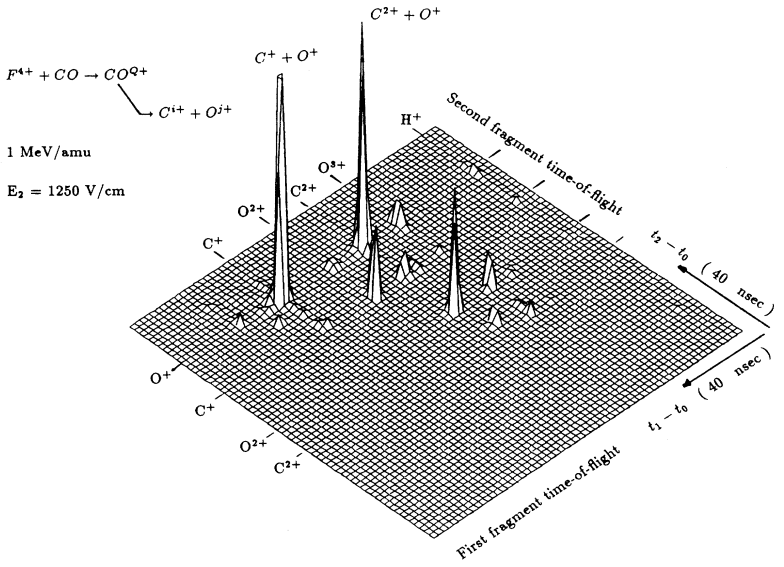

FIG. 3. Coincidence TOF spectrum of CO fragmentation, produced by F^{4+} impact at 1 MeV/amu, measured with a strong extraction field of 1250 V/cm. The $C^+ + O^+$ peak is truncated so that the smaller fragmentation channels can be seen.

TABLE I. The abundances of final products where only one ion was produced (single fragment) by 1-MeV/amu F^{4+} relative to CO^+.

Channels	Relative cross sections (%)	Relative errors (%)
CO^+	100.00±0.21	0.2
CO^{2+}	1.42±0.13	9.2
C^0+O^+	13.9±1.4	10.1
$C^+ + O^0$	15.9±1.4	8.8
C^0+O^{2+}	1.56±0.28	17.9
$C^{2+}+O^0$	3.29±0.48	14.6
C^0+O^{3+}	0.176±0.042	23.9
$C^{3+}+O^0$	0.477±0.078	16.4
C^0+O^{4+}	0.0147±0.0055	37.4
$C^{4+}+O^0$	0.0490±0.018	22.4

TABLE II. The abundances of ion-pair final products produced by 1-MeV/amu F^{4+} relative to $C^+ + O^+$ breakup. The numbers in parentheses are the uncertainties (in %).

	O^+	O^{2+}	O^{3+}	O^{4+}	O^{5+}	O^{6+}
C^+	100.0 ±4.9 (4.9%)	12.69 ±0.67 (5.3%)	1.227 ±0.089 (7.2%)	0.38 ±0.12 (31.6%)	0.0207 ±0.0056 (27.0%)	0.0046 ±0.0020 (43.5%)
C^{2+}	30.9 ±1.6 (5.2%)	14.99 ±0.74 (4.9%)	2.23 ±0.12 (5.4%)	0.588 ±0.043 (7.3%)	0.140 ±0.017 (12.1%)	0.0276 ±0.0050 (18.1%)
C^{3+}	3.40 ±0.18 (5.3%)	4.11 ±0.20 (4.9%)	1.23 ±0.062 (5.0%)	0.201 ±0.0023 (11.4%)	0.0770 ±0.0098 (12.7%)	0.0170 ±0.0034 (20.0%)
C^{4+}	0.224 ±0.020 (8.9%)	0.488 ±0.039 (8.0%)	0.218 ±0.018 (8.2%)	0.0333 ±0.0037 (11.1%)	0.0110 ±0.0026 (23.6%)	0.0029 ±0.0014 (48.3%)
C^{5+}			0.002 01 ±0.000 56 (27.9%)	0.00119 ±0.000 45 (37.8%)	0.00069 ±0.000 40 (58.0%)	

TABLE III. The abundances of single-ion and ion-pair final products produced by 1-MeV/amu F^{4+} relative to CO^+. The numbers in parentheses are the uncertainties (in %).

	O^0	O^+	O^{2+}	O^{3+}	O^{4+}	O^{5+}	O^{6+}
C^0		13.9 ±1.4 (10.1%)	1.56 ±0.28 (17.9%)	0.176 ±0.042 (23.9%)	0.0147 ±0.0055 (37.4%)		
C^+	15.9 ±1.4 (8.8%)	17.5 ±1.9 (10.8%)	2.22 ±0.24 (10.8%)	0.214 ±0.025 (11.7%)	0.066 ±0.023 (33.3%)	0.0036 ±0.0010 (27.8%)	0.000 80 ±0.00 35 (43.8%)
C^{2+}	3.29 ±0.48 (14.6%)	5.41 ±0.57 (10.5%)	2.62 ±0.28 (10.7%)	0.389 ±0.042 (10.8%)	0.103 ±0.012 (11.6%)	0.0245 ±0.0037 (15.1%)	0.004 82 ±0.000 99 (20.5%)
C^{3+}	0.477 ±0.078 (16.4%)	0.594 ±0.064 (10.8%)	0.718 ±0.076 (10.6%)	0.215 ±0.023 (10.7%)	0.0352 ±0.0052 (14.8%)	0.0135 ±0.0021 (15.6%)	0.002 96 ±0.000 66 (22.3%)
C^{4+}	0.0490 ±0.018 (22.4%)	0.0392 ±0.0051 (13.0%)	0.0853 ±0.011 (11.7%)	0.0382 ±0.0048 (12.6%)	0.005 83 ±0.000 84 (14.4%)	0.001 93 ±0.000 48 (25.3%)	0.000 51 ±0.000 25 (49.0%)
C^{5+}				0.000 35 ±0.000 10 (29.7%)	0.000 208 ±0.000 081 (38.4%)	0.000 120 ±0.000 071 (58.4%)	

same integrated beam current N_p and the same target pressure. Thus the CO^+ production cross section is given by

$$\sigma(CO^+)=\sigma(Ne^+)\times\frac{S^{\text{meas}}(CO^+)}{S^{\text{meas}}(Ne^+)} . \quad (4)$$

The total cross section for Ne^+ production by 1-MeV/amu F^{4+} projectiles is $\sigma(Ne^+)=(4.3\pm1.3)\times10^{-16}$ cm^2 as measured by Heber *et al.* [16]. Thus the total cross section for CO^+ production is

$$\sigma(CO^+)=(1.7\pm0.8)\times10^{-15}\ cm^2 . \quad (5)$$

Finally, the total cross sections of all CO final products produced by 1-MeV/amu F^{4+} impact can be evaluated by multiplying the relative abundances given in Table III by the CO^+ total cross section given in Eq. (5).

IV. RESULTS AND DISCUSSION

The formation of a highly charged intermediate molecular state and its dissociation into fragments can be expressed by the following equation:

$$F^{4+}+CO\rightarrow CO^{Q+*}\rightarrow \begin{cases} CO^{Q+} \\ C^{i+}+O^{j+} \end{cases} . \quad (6)$$

The only molecular ions detected were CO^+, which is the main product, and CO^{2+}. Most of the CO^{2+}* formed in the collision breaks up rapidly and only a small fraction, about 6.0±0.7 % of the total CO^{2+} production deexcites to a stable or metastable state of CO^{2+}. This branching ratio was evaluated using all CO^{2+} final products tabulated in Table III i.e.,

$$[CO^{2+}]/([C^{2+},O]+[C^+,O^+]+[C,O^{2+}]+[CO^{2+}]) .$$

Molecular ions having charge states higher than 2 were not detected indicating that they dissociate faster than the extraction time which is of the order of 100 nsec for CO^{3+}. (Extraction time is defined as the time for the ion

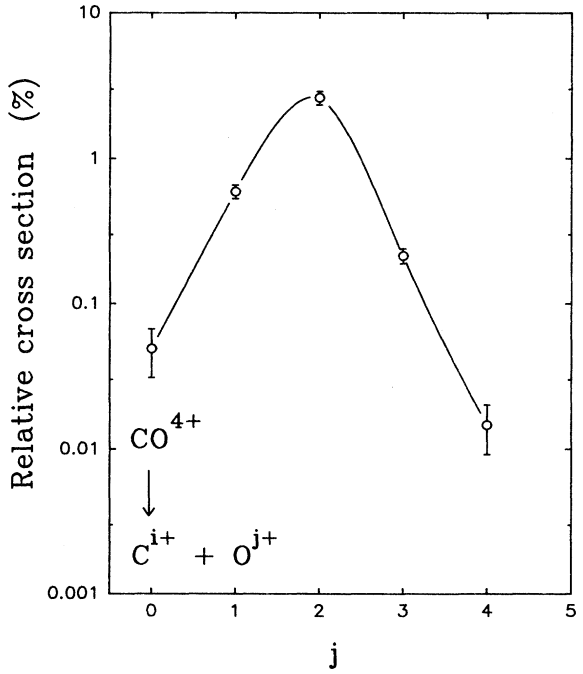

FIG. 4. Fragmentation pattern of $CO^{4+}\rightarrow C^{i+}+O^{j+}$ produced by 1-MeV/amu F^{4+} impact as a function of the number of vacancies on the oxygen j. The dashed line is a spline fit to guide the eye.

to travel from the point of formation to the field free region. If the molecule dissociates in the drift region its fragments will have the same time of flight as the parent molecular ion. Total time of flight is of the order of microseconds.)

The electrons of the CO^{Q+*} molecular ion rearrange rapidly in a way which favors breakup channels with approximately the same number of vacancies on each fragment, even though the CO molecule is heteronuclear, as can be seen from the fragmentation pattern of CO^{4+} shown in Fig. 4. The lower ionization potential of C^{j+} relative to O^{j+} causes a slight asymmetry in the distribution, because removing an electron from the carbon is more likely than from the oxygen for the same charge state. To further test this feature in a quantitative way we have calculated the average charge state of the oxygen fragment for each number of electrons removed. This average value $\bar{j}$ is plotted in Fig. 5 as a function of the number of electrons removed. The solid line in the figure represents symmetric breakup, i.e., $\bar{j}=Q/2$. It can be seen that up to $Q\sim 6$ the experimental values follow the $\bar{j}=Q/2$ relationship. In order for $\bar{j}=Q/2$ to remain valid for $Q\geq 7$, breakup channels in which a K-shell electron of the carbon target is removed would have to occur with a similar probability as removing the same number of electrons from the oxygen L shell. Due to the large ionization potential difference between the K shell and L shell, however, K-shell electron removal is much less likely. The $\bar{j}$ curve therefore deviates from $\bar{j}=Q/2$ for $Q\geq 7$. Even though the breakup probability peaks approximately at $\bar{i}\sim\bar{j}$ there are systematic deviations from symmetry, e.g., the $C^{i+}+O^{j+}$ is typically more likely to happen than the $C^{j+}+O^{i+}$ channel if $i>j$. This is due to the lower ionization potentials of the carbon ions in comparison with the oxygen ions of the same charge state.

The breakup into a neutral fragment and a charged fragment decreases rapidly with increasing number of electrons removed as shown in Fig. 6. The cross section for $C^{Q+}+O$ is always much larger than the cross section

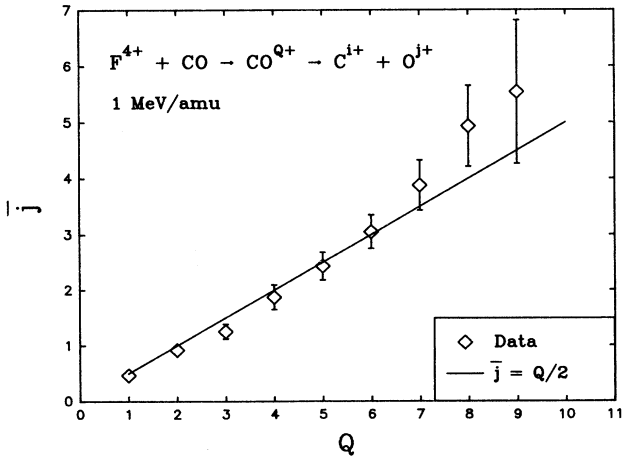

FIG. 5. Average charge state of the oxygen fragment produced by 1-MeV/amu F^{4+} impact as a function of the number of electrons removed Q. The solid line represents $\bar{j}=Q/2$.

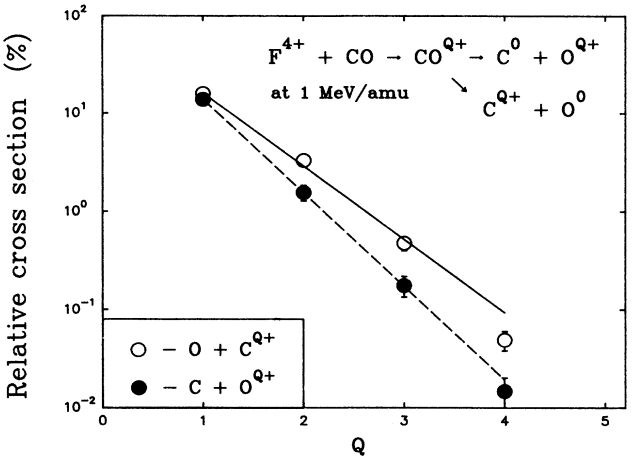

FIG. 6. Cross sections for removing all the electrons from either the carbon or the oxygen by 1-MeV/amu F^{4+} impact relative to the CO^{+} cross section, as a function of the number of electrons removed Q. The lines represent an exponential fit to the data: ——, $C^{Q+}=16.1e^{-1.72Q}$; — — —, $O^{Q+}=13.9e^{-2.19Q}$.

for $C+O^{Q+}$ due to the ionization potential differences discussed above. This effect has been recently reported by Becker *et al.* [17] for photoionization of CO in which the $C^{+}+O^{*}$ is more likely than $C^{*}+O^{+}$ as an intermediate state leading to $C^{+}+O^{+}$ breakup. The errors in the channels increase rapidly because the lost-fragment contribution becomes comparable or even larger than the neutral channel itself.

The cross sections for removing Q electrons can be calculated by summing all the cross sections in Table III which have Q electrons missing. These multiple-electron removal cross sections relative to the single electron-removal cross section $\sigma(CO^{+*})$ are plotted in Fig. 7. Relative cross sections for electron removal from an

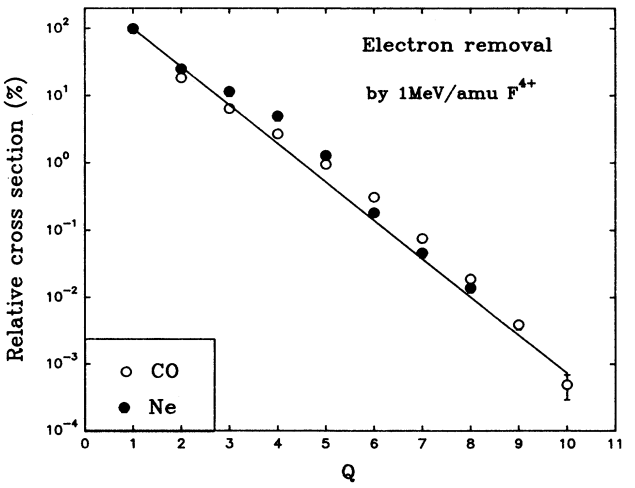

FIG. 7. Cross sections for removing electrons from either CO or Ne, by 1-MeV/amu F^{4+} impact, relative to the singly charged CO^{+} and Ne^{+} cross section, respectively, as a function of the number of electrons removed Q. The line represents an exponential fit to the CO data: ——, $100e^{-1.31Q}$.

atomic Ne target by similar collisions are plotted for comparison. The cross sections for electron removal decrease rapidly with increasingly Q for both targets. These relative cross sections fall off approximately as the exponential $e^{-1.3Q}$. The total electron-removal cross sections from the CO target are larger than from the Ne target as expected because of the lower ionization potential and the larger number of valence electrons. Even though the total electron-removal cross sections from CO and Ne differ systematically, the two targets have similar relative cross sections for removal of a few electrons. This is in agreement with independent-electron approximation calculations [18], which predict that for collisions where multiple ionization is significant, the relative ionization cross sections are independent of the number of equivalent electrons. We intend to further investigate this trend by measuring other targets with different numbers of valence electrons.

V. CONCLUSIONS

Molecular fragmentation of the CO diatomic molecule induced by 1-MeV/amu F^{4+} impact has been investigated using the coincidence time-of-flight spectroscopy technique. In these collisions, multiply charged CO^{Q+*} molecular ions are produced. These unstable molecular ions rapidly dissociate into fragments having relatively high kinetic energies. The production cross sections of all final products have been determined. The main product was the singly charged molecular ion CO^+. The only other molecular ion detected was the doubly charged CO^{2+} molecular ion. Electron-removal cross sections, i.e., intermediate-charge-state production cross sections, decrease rapidly with increasing number of electrons removed. These cross sections relative to the single electron-removal cross section are similar to the same cross sections for Ne^{Q+*} production, especially for removal of a few electrons, in agreement with independent-electron approximation calculations.

The breakup of each intermediate charge state CO^{Q+*} peaks at the breakup channel for which both fragments have an equal number of vacancies, as long as no K-shell electrons are removed. Systematically, there are more vacancies on the carbon than on the oxygen both in neutral channels and in ion-pair channels. This is due to the lower ionization potentials of the carbon ions.

ACKNOWLEDGMENTS

We thank Professor L. Weaver for numerous stimulating and enlightening discussions. This work was supported by the Office of Basic Energy Sciences, U.S. Department of Energy.

APPENDIX

Data analysis necessary for the evaluation of single-fragment and ion-pair production cross sections needs to be done in a self-consistent way described below. In the following section a set of equations is derived for the evaluation of the true number of events occurring in the target cell during the experiment. The method for solving these equations and reducing the errors in the relative abundances is discussed in Sec. 2.

1. Evaluation of the true number of single fragments and ion pairs

The number of counts in each coincidence and singles peak is proportional to the production cross section of the relevant breakup channel. In order to calculate these cross sections we have to know the efficiency for detection of both fragments in coincidence and the efficiency for detection of a single ion. A strong extraction field $\mathcal{E}_2=1250$ V/cm was used for the production cross-section measurement. Under these conditions all fragments which passed the exit collimator were detected except for those lost on the meshes or on the detector itself. The detection efficiency for a neutral channel, for example $CO^{Q+}\rightarrow C^{i+}+O^0$, is simply given by the detection probability of the charged ion

$$\epsilon_r=\epsilon_d T^4 , \tag{A1}$$

where ϵ_d is the detector efficiency and T is the transmission through one of the four identical high transmission meshes. The efficiency of microchannel plate detectors increases with ion energy and levels off at about 3 keV for all ions to a value which is the open area of the detector (i.e., the ratio of the area of the open channels to the total area of the first plate) as reported by Gao *et al.* [19]. The detector used has an open area of 55%, which was assumed to be the detection efficiency ϵ_d for all ions since their energy was above 5 keV. The meshes used have 90% transmission.

The detection efficiency for a coincidence channel $CO^{Q+}\rightarrow C^{i+}+O^{j+}$ can be written as the product of the independent detection probability of each ion ϵ_r and the dependent extraction probability of both ions η_{ij} as follows:

$$\epsilon_{ij}=\eta_{ij}\epsilon_r^2 , \tag{A2}$$

where η_{ij} is the ion-pair extraction probability, i.e., the probability that both fragments will get through the exit collimator. (Hereafter, the subscripts i and j are used for C^{i+} and O^{j+}, respectively.)

The ion-pair extraction probability of both fragments in a $C^{i+}+O^{j+}$ two-body breakup to exit through the collimator as a function of their kinetic energy, E_k, and charge states was evaluated in closed form for the TOF spectrometer used in these measurements [12]. This probability $\eta_{ij}(E_k)$ is given by

$$\eta_{ij}(E_k)=1-\frac{1}{2w\mathcal{E}_2}\left[\frac{E_i}{q_i}\frac{1}{k_i}F(\tfrac{3}{2};-\tfrac{1}{2};2;k_i^2)+\frac{E_j}{q_j}\frac{1}{k_j}F(\tfrac{3}{2};-\tfrac{1}{2};2;k_j^2)\right] , \tag{A3}$$

where $k_i^2=1/(1+d_c q_i \mathcal{E}_2/E_i$, $k_j^2=1/(1+d_c q_j \mathcal{E}_2/E_j)$, $E_k=E_i+E_j$ is the kinetic energy released in the breakup, $E_{i,j}$ and $q_{i,j}$ are the kinetic energy and charge state of each ion, d_c is the distance between the exit collimator and the beam axis, and w is the exit collimator half width. The ion-pair extraction probability $n_{ij}(E_k)$ must be evaluated separately for each breakup channel because it depends strongly on the kinetic energy and charge states of the fragments.

The kinetic-energy distribution of each breakup channel was evaluated by fitting the time-difference spectrum with a simulated spectrum produced by those fragments having a Gaussian kinetic-energy distribution around $\overline{E_k}$, as shown in Fig. 8. This method is commonly used in photoion-photoion-coincidence measurements [3–5]. These ion-pair extraction probabilities η_{ij}, for most channels, were large, for example, $\eta_{ij}=0.913$ for $C^{2+}+O^+$ breakup, which has a measured average breakup energy of the order of 20 eV. The large ion-pair extraction probabilities reduce the uncertainty in the cross sections evaluated. Recently, anisotropies in the angular distributions were reported [20,21] for some collision systems. On the other hand Ezell *et al.* [22] reported that double ionization of H_2 molecules by fast H^+ impact is isotropic. For a strong extraction field all ions are extracted, independent of the orientation of the molecule before the breakup, from most of the target length. Fragments are lost only in a small region close to the aperture edge. Thus the effect of anisotropies on the ion-pair extraction efficiency, which is typically above 85%, is less than a few percent.

Further complications exist in the evaluation of the detection efficiency of breakup channels for which the time-of-flight difference is small. A minimum separation time of 11 nsec between the two fragments is needed in order to record such coincidence events. Thus only a small fraction of the $C^{3+}+O^{4+}$ and the $C^{4+}+O^{5+}$ breakup events are recorded. Only molecular ions which are aligned within a narrow cone whose axis is parallel to the extraction field have a large enough time difference to be recorded. Thus the detection probability of these channels can be written as a product of the detection efficiency n_{ij}, given in Eq. (A2), and the fraction of ion pairs whose time difference was larger than 11 nsec, μ_{34} and μ_{45}.

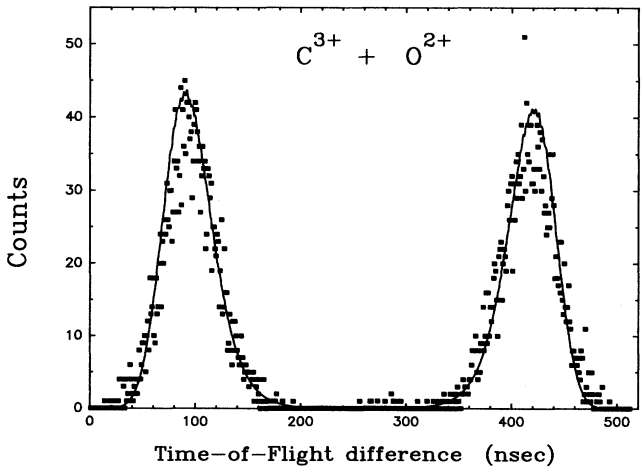

FIG. 8. Time-difference spectrum of the $CO^{3+}\rightarrow C^{2+}+O^+$ breakup channel produced by 1-MeV/amu F^{4+} impact. The extraction field was 156 V/cm. Data (■), simulated spectrum with $\overline{E_k}=40$ eV and full width at half maximum $=30$ eV (——).

In order to evaluate the cross sections of all single-fragment and ion-pair breakup channels from the areas measured from Figs. 2 and 3 some corrections have to be made beyond the correction for the different detection efficiencies of the different channels. The main corrections are random coincidences, lost-fragments, and ions from contaminants in the target gas. The lost-fragment correction is needed because in some of the events where an ion pair was produced in a single collision, such as $C^{i+}+O^{j+}$, only one of them was detected. In these events where an ion pair is produced there is a certain probability of detecting both of them ϵ_{ij}, which is given by Eq. (A2). There is also a certain probability of detecting only one of the two fragments while the other fragment is stopped by the meshes or hits the detector in the nonactive area. If one fragment was not detected a single ion will be recorded in Fig. 2 even though it was an ion-pair event which should have been recorded as a coincidence in Fig. 3. The probability of losing one fragment out of two, while detecting the other, is given by

$$\epsilon_r P_{1of2}(i,j)=\eta_{ij}\epsilon_r(1-\epsilon_r)+(1-\eta_{ij})\epsilon_r \ , \tag{A4}$$

where $P_{1of2}(i,j)$ is the probability of losing one fragment. The first term in Eq. (A4) is the probability for losing one fragment on the detector or meshes after both fragments made it through the exit collimator, and the second term is the probability of losing one fragment on the exit collimator. The effect of lost fragments is the main contributor to the highly charged fragments in the single spectrum as the fragmentation of a highly charged CO into a neutral and a highly charged fragment is very unlikely.

Another important correction is needed because of random coincidences caused by two collisions occurring within the same beam bunch. Although the experiment was performed in single collision conditions (i.e., a linear pressure dependence of the CO^+ count rate), there is always a small probability of double collisions. This rate of double collisions was very small, but so was the true coincidence rate of some channels. The measured number of random coincidence counts $C_R^{\rm meas}(i,j)$ caused by two neutral channels is given by

$$C_R^{\rm meas}(i,j)=\tau S^{\rm meas}(i)S^{\rm meas}(j) \ , \tag{A5}$$

where $S^{\rm meas}(i)$ and $S^{\rm meas}(j)$ are the number of counts of the two single-fragment channels and τ is the random coincidence coefficient. This random coincidence coefficient can be evaluated directly from the data by using coincidence channels which are purely random, for example the coincidence of CO^{2+} with CO^+ which can

be produced only by a random coincidence. For this example, τ is given by

$$\tau=\frac{C^{\text{meas}}(CO^{2+},CO^{+})}{S^{\text{meas}}(CO^{2+})S^{\text{meas}}(CO^{+})}=(3.59\pm0.04)\times10^{-9}\ , \tag{A6}$$

where $C^{\text{meas}}(CO^{2+},CO^{+})$ is the number of counts of CO^{2+} in coincidence with CO^{+} and $S^{\text{meas}}(CO^{2+})$ and $S^{\text{meas}}(CO^{+})$ are the number of counts of CO^{2+} and CO^{+} singles, respectively. The random coincidence coefficient was evaluated for a few purely random coincidence channels. The value used for the data reduction was the average value of this sample $\bar{\tau}$ while twice the standard deviation determined the error associated with it, thus $\bar{\tau}=(3.4\pm0.6)\times10^{-9}$.

Finally, some contaminants in the target gas, mainly N_2, O_2, and H_2O, have to be subtracted from both single-fragment and coincidence channels. These contaminants were subtracted using data of F^{4+} colliding with these targets under the same conditions, and normalizing it to the H_2O^{+} and O_2^{+} singles in the $F^{4+}+CO$ run. For the clarity of the discussion hereafter the background contribution is not included in the yield equations even though they were included in the data reduction.

As discussed above the breakup channels producing one ion and the ones producing ion pairs contribute to counts in both the single-fragment and coincidence spectra. In order to calculate the true number of events in each breakup channel we have to solve a set of nonlinear coupled equations. The coupling strength depends strongly on the values of η_{ij}, ϵ_r, and $\bar{\tau}$. The equations describing the measured number of singles, for example the number of C^{i+} single ions $S^{\text{meas}}(C^{i+})$ are given by

$$S^{\text{meas}}(C^{i+})=\epsilon_r S(C^{i+})+\sum_j \epsilon_r P_{1\text{of}2}(i,j)C(C^{i+},O^{j+})\ , \tag{A7}$$

where $S(C^{i+})$ is the true number of C^{i+} single-ion events, $C(C^{i+},O^{j+})$ is the true number of $C^{i+}+O^{j+}$ ion-pair events, and $\epsilon_r P_{1\text{of}2}(i,j)$ is the probability of detecting one fragment out of two which is given in Eq. (A4). Double-collision contributions to the single rates were not included because they are negligible in comparison with the lost-fragment correction. Similar equations describe all the other single-fragment channels measured. The equations describing the measured number of $C^{i+}+O^{j+}$ coincidences $C^{\text{meas}}(C^{i+},O^{j+})$ is given by

$$\begin{aligned}C^{\text{meas}}(C^{i+},O^{j+})=&\eta_{ij}\epsilon_r^2 C(C^{i+},O^{j+})+\bar{\tau}\epsilon_r^2 S(C^{i+})S(O^{j+})+\bar{\tau}\epsilon_r^2\sum_k P_{1\text{of}2}(k,j)S(C^{i+})C(C^{k+},O^{j+})\\&+\bar{\tau}\epsilon_r^2\sum_l P_{1\text{of}2}(i,l)C(C^{i+},O^{l+})S(O^{j+})+\bar{\tau}\epsilon_r^2\sum_k\sum_l P_{1\text{of}2}(i,l)P_{1\text{of}2}(k,j)C(C^{i+},O^{l+})C(C^{k+},O^{j+})\ .\end{aligned} \tag{A8}$$

Special care has to be taken when calculating breakup channels in which one of the ions is either C^{3+} or O^{4+} because they are not resolved in the single-fragment spectrum and are only partly resolved in some of the coincidence channels. For simplicity all contributions due to background and special cases like the one discussed above were omitted from Eq. (A8).

These sets of nonlinear coupled equations describe the number of detected recoils in each channel. The single-fragment events described by Eq. (A7) include the molecular ions CO^{+} and CO^{2+} and all the breakup channels in which one fragment is neutral, i.e., $C^{i+}+O$ and $C+O^{j+}$. Thirteen such equations were required to describe the channels measured with adequate statistics. The coincidence events described by Eq. (A8) include all the ion-pair breakup channels $C(C^{i+},O^{j+})$. There are twenty-seven such coincidence equations for which enough counts were measured. This large set of nonlinear equations can be solved by iteration, as described in the next section [using Eqs. (A11) and (A12)], in order to find the number of true single-fragment events as well as the number of true ion-pair events. The coupling constants of these equations ϵ_r, τ, and η_{ij}, are determined independently as described earlier. The main contribution to the errors in the relative abundances evaluated using these equations is the uncertainty in the recoil ion detection efficiency, which is known to be the same for all recoil ions in our measurements but has a relatively large uncertainty in the exact value. A method which minimizes the effect of this uncertainty in ϵ_r on the relative abundances is discussed in the next section, together with the details of the solution method used.

2. Equations solution and error reduction method

As discussed above the recoil ion detection efficiency is known to be the same for all recoil ions in our measurements, but there is a relatively large uncertainty in its exact value. Thus, it is convenient to solve the equations above for $S_e(C^{i+})=\epsilon_r S(C^{i+})$ and $C_e(C^{i+},O^{j+})=\epsilon_r^2 C(C^{i+},O^{j+})$ instead of for the true number of events because it reduces the influence of the error in ϵ_r on the relative abundances of all breakup channels. Now rewriting Eq. (A7) and Eq. (A8) for the new variables yields the following set of nonlinear coupled equations for single ions

$$S_e(C^{i+})=S^{\text{meas}}(C^{i+})-\frac{1}{\epsilon_r}\sum_j P_{1\text{of}2}(i,j)C_e(C^{i+},O^{j+})\ , \tag{A9}$$

and for the ion pairs

$$C_e(C^{i+},O^{j+})=\frac{1}{\eta_{ij}}\left\{C^{\text{meas}}(C^{i+},O^{j+})-\bar{\tau}S_e(C^{i+})S_e(O^{j+})-\frac{\bar{\tau}}{\epsilon_r}\sum_k P_{1\text{of}2}(k,j)S_e(C^{i+})C_e(C^{k+},O^{j+})\right.$$
$$-\frac{\bar{\tau}}{\epsilon_r}\sum_l P_{1\text{of}2}(i,l)C_e(C^{i+},O^{l+})S_e(O^{j+})$$
$$\left.-\frac{\bar{\tau}}{\epsilon_r^2}\sum_k\sum_l P_{1\text{of}2}(i,l)P_{1\text{of}2}(k,j)C_e(C^{i+},O^{l+})C_e(C^{k+},O^{j+})\right\}. \quad \text{(A10)}$$

In these new sets of nonlinear coupled equations the recoil ion detection efficiency ϵ_r appears only in the correction terms due to lost fragments and random coincidences, which are much smaller than the number of counts for most channels. Furthermore, in the ion-pair equations the ϵ_r^2 term appears only for the two ion-pair production term which is the smallest double-collision contribution. Thus $S_e(C^{i+})$ and $C_e(C^{i+},O^{j+})$ can be evaluated more precisely than $S(C^{i+})$ and $C(C^{i+},O^{j+})$ because the uncertainty in ϵ_r, which is the main error in equations (A7) and (A8), has a smaller effect on equations (A9) and (A10). This uncertainty in the recoil detection efficiency ϵ_r is mostly due to the unknown fraction of recoil signals which are below the discriminator level (i.e., the detector efficiency might be somewhat smaller than the detector open area fraction).

Now, the set of nonlinear coupled equations (A9) and (A10) can be solved by iteration. First, S_e and C_e are set equal to the measured number of counts S^{meas} and C^{meas}, respectively. Then the equations are used to evaluate the next values of S_e

$$S_e^{(n+1)}(C^{i+})=S^{\text{meas}}(C^{i+})-\frac{1}{\epsilon_r}\sum_j P_{1\text{of}2}(i,j)C_e^{(n)}(C^{i+},O^{j+}), \quad \text{(A11)}$$

and C_e

$$C_e^{(n+1)}(C^{i+},O^{j+})=\frac{1}{\eta_{ij}}\left\{C^{\text{meas}}(C^{i+},O^{j+})-\bar{\tau}S_e^{(n)}(C^{i+})S_e^{(n)}(O^{j+})-\frac{\bar{\tau}}{\epsilon_r}\sum_k P_{1\text{of}2}(k,j)S_e^{(n)}(C^{i+})C_e^{(n)}(C^{k+},O^{j+})\right.$$
$$-\frac{\bar{\tau}}{\epsilon_r}\sum_l P_{1\text{of}2}(i,l)C_e^{(n)}(C^{i+},O^{l+})S_e^{(n)}(O^{j+})$$
$$\left.-\frac{\bar{\tau}}{\epsilon_r^2}\sum_k\sum_l P_{1\text{of}2}(i,l)P_{1\text{of}2}(k,j)C_e^{(n)}(C^{i+},O^{l+})C_e^{(n)}(C^{k+},O^{j+})\right\}. \quad \text{(A12)}$$

A solution is reached after a few iterations. The condition used for convergence was $|S_e^{(n+1)}-S_e^{(n)}|<1$ and $|C_e^{(n+1)}-C_e^{(n)}|<1$. The sensitivity of the solution to variation of the coupling constants η_{ij}, $\bar{\tau}$, and ϵ_r was checked and is included in the error bars. The direct evaluation of $\bar{\tau}$ from the pure random coincidences in each run minimizes its effect on the relative abundances uncertainties. On the other hand, the uncertainty in ϵ_r is a major contributor to the errors in most relative cross sections.

[1] K. E. McCulloh and H. M. Rosenstock, J. Chem. Phys. **48**, 2048 (1968).
[2] B. Brehm and G. de Frenes, Int. J. Mass Spectrom. Ion Phys. **26**, 251 (1978).
[3] P. Lablanquie, J. Delwiche, M.-J. Franskin-Hubin, I. Nenner, J. H. D. Eland, and K. Ito, J. Mole. Struc. **174**, 141 (1988).
[4] P. Lablanquie, J. Delwiche, M.-J. Franskin-Hubin, I. Nenner, P. Morin, K. Ito, J. H. D. Eland, J.-M. Robbe, G. Gandara, J. Fournier, and P. G. Fournier, Phys. Rev. A **40**, 5673 (1989).
[5] A. P. Hitchcock, P. Lablanquie, P. Morin, E. Lizon, A. Lugrin, M. Simon, P. Thirty, and I. Nenner, Phys. Rev. A **37**, 2448 (1988).
[6] A. K. Edwards and R. M. Wood, J. Chem. Phys. **76**, 2938 (1982).
[7] M. B. Shah and H. B. Gilbody, J. Phys. **23**, 1491 (1990).
[8] C. L. Cocke, Phys. Rev. A **20**, 749 (1979).
[9] H. Tawara, Phys. Rev. A **33**, 1385 (1986).
[10] G. Sampoll, O. Heber, R. J. Maurer, P. A. Scott, and R. L. Watson, Nucl. Instrum. Methods **B40/41**, 308 (1989).
[11] G. Sampoll, R. L. Watson, O. Heber, V. Horvat, K. Wohrer and M. Chabot, Phys. Rev. A **45**, 2903 (1992).
[12] I. Ben-Itzhak, S. G. Ginther, and K. Carnes, Nucl. Instrum. Methods **B66**, 401 (1992).
[13] W. C. Wiley and I. H. McLaren, Rev. Sci. Instrum. **26**, 1150 (1955).
[14] J. Ullrich and H. Schmidt-Böcking, Phys. Lett. A **125**, 1931 (1987).
[15] T. J. Gray, C. L. Cocke, and E. Justiniano, Phys. Rev. A **22**, 849 (1980).
[16] O. Heber *et al.* (unpublished).

[17] U. Becker, O. Hemmers, B. Langer, A. Menzel, R. Wehlitz, and W. B. Peatman, Phys. Rev. A **45**, R1295 (1992).
[18] I. Ben-Itzhak, T. J. Gray, J. C. Legg, and J. H. McGuire, Phys. Rev. A **37**, 3685 (1988).
[19] R. S. Gao, P. S. Gibner, J. H. Newman, K. A. Smith, and R. F. Stebbings, Rev. Sci. Instrum. **55**, 1758 (1984).
[20] S. L. Varghese, C. L. Cocke, S. Cheng, E. Y. Kamber, and V. Frohne, Nucl. Instrum. Methods **B40/41**, 266 (1989).
[21] S. Cheng, C. L. Cocke, V. Frohne, E. Y. Kamber, and S. L. Varghese, Nucl. Instrum. Methods **B56/57**, 78 (1991).
[22] R. L. Ezell, A. K. Edwards, R. M. Wood, M. W. Dittmann, J. F. Browning, and M. A. Mangan, Nucl. Instrum. Methods **B56/57**, 292 (1991).